Nanostructured CMOS Wireless Ultra-Wideband Label-free DNA Analysis SoC

H. M. Jafari[1], L. Soleymani[2], K. Abdelhalim[1], E. H. Sargent[1], S. O. Kelley[1] and R. Genov[1]
1. University of Toronto, Toronto, ON, CANADA, 2. McMaster University, Hamilton, ON, CANADA

Abstract

A 0.13-micron CMOS fully integrated 48-channel UWB label-free DNA analysis SoC is demonstrated in prostate cancer screening. The 3mm×3mm die includes 578 nanostructured DNA sensors, 48 pH sensors, and 48 temperature sensors and reuses key circuits for cyclic voltammetry, amperometry and temperature regulation.

Introduction

Amperometric electrochemical DNA sensors [1] have emerged as a low-cost, high-throughput and real-time alternative to conventional optical and electrochemical sensory methods [2]. We have reported in Nature Nanotechnology amperometric electrochemical sensors fabricated on passive silicon that do not require cumbersome tagging of DNA with chemical or optical labels [3]. These gold microelectrodes have fine-tuned nanostructured patterns on their surface that yield an over 110dB input dynamic range and 1aM sensitivity sufficient for PCR-free DNA detection. In this paper we present a 0.13μm CMOS DNA analysis SoC with 578 nanostructured gold microelectrodes grown directly on the die which performs label-free DNA analysis, pH sensing and temperature regulation for cancer detection.

System Description

The nanostructured gold microelectrodes are electrostatically grown on a Ni/Pd/Au base on the CMOS top metal as depicted in Fig. 1 (center). The dynamic range and sensitivity are a function of the electrode nanostructure grain size, shape and degree of anisotropy which are controlled by the potential difference between the working electrode (WE) and a Ag/AgCl reference electrode as shown in Fig. 1 (middle and bottom). Potassium ferrocyanide reporter $K_4[Fe(CN)_6]$ is utilized as a redox chemical current generator, as depicted in Fig. 1 (top) for the case of oxidization. The oxidization current I_{OX} drops when the Au electrode surface is hybridized with negatively charged probe DNA. When the complementary DNA binds with the probe DNA, the surface negative charge further increases and the oxidization current is further reduced. This change in the current is a key indicator of the target DNA presence and concentration.

The block diagram of the SoC is presented in Fig. 2 (top, left). Three current-mode sensors: an array of nanostructured DNA sensors, a pH sensor and a CTAT/PTAT temperature sensor, share each of 48 signal acquisition channels. The dual-slope multiplying ADC (MADC) generates a digital representation of the product of an analog input current and a digital coefficient. Accumulation is implemented by an extended ADC counter. As a result, a digital multiplier and an accumulator are eliminated. As shown in Fig. 2, the channel circuits are reused to implement three commonly required sensory modalities: a) cyclic voltammetry (CV) for DNA sensing, b) constant-potential amperometry (CPA) for pH sensing, and c) temperature regulation.

The circuit implementation of one channel is depicted in Fig. 3 (top). The type-II bi-directional input current conveyer

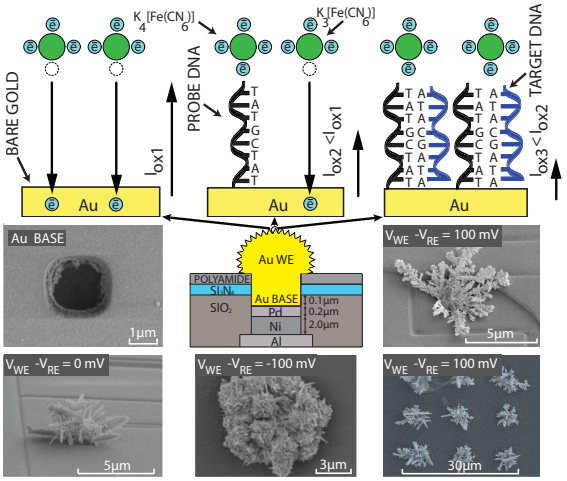

Fig. 1. On-CMOS nanostructured label-free DNA microsensors.

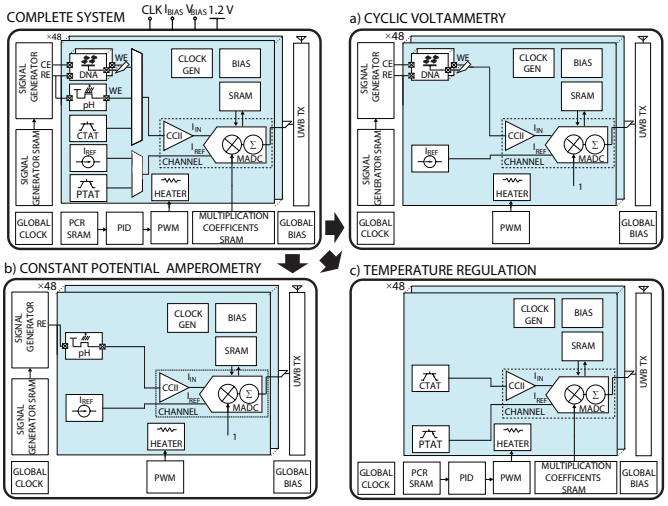

Fig. 2. SoC architecture resources reuse in three modes of operation.

is chopper-stabilized internally. Its output current mirrors are regulated and dynamically matched. Low-leakage switches are utilized. The MADC employs three gain stages with the first stage chopper-stabilized. Multiplication of the input current by a digital coefficient $0 < M < 1$ is implemented by scaling the duration of the charging phase in the counter by M, which requires no additional resources [4]. The pulsed UWB transmitter modulates Manchester-encoded input data using on-off keying as shown in Fig. 3 (bottom, right).

The temperature sensing and regulation circuits are shown in Fig. 4. In-channel PTAT and CTAT BJTs share common peripheral circuits to generate two currents as the input and reference currents to the MADC, respectively. The difference between these currents is proportional to the temperature. Temperature regulation is implemented by a mixed-signal PID feedback controller. The PID controller compares the programmed desired temperature value with the measured temperature and adjusts the duty cycle of the fully digital 12-bit pulse

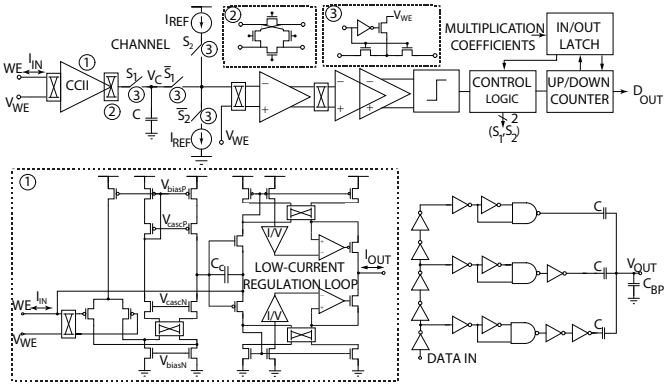

Fig. 3. VLSI circuit implementation of the channel and UWB TX.

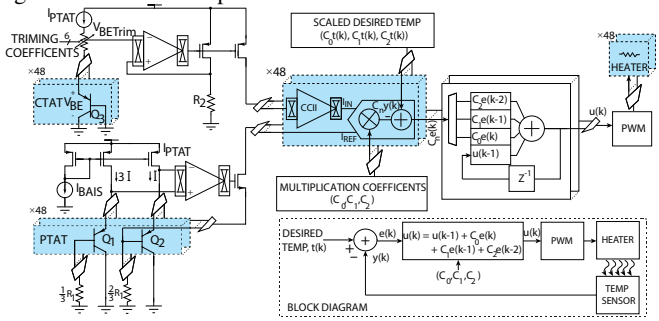

Fig. 4. Circuit implementation of the temperature regulator.

width modulator (PWM). The PWM controls the in-channel heater to deliver an average power necessary to maintain the desired temperature.

Experimental Results

The static digital output of one channel for three clock frequencies is depicted in Fig. 5(a). Fig. 5(b) shows the FFT of the measured ADC output at 12MHz clock with ENOB of 9.1. The combined linear input dynamic range is 110dB. The in-channel pH sensor is implemented by a floating gate PFET with an aspect ratio of 0.5/6μm. The sensitivity of the ISFET to pH of liquids and the 3σ error bars (from 3 chips) are shown in Fig. 5(c). The inaccuracy of the temperature regulation after calibration is $\pm$0.5 C as depicted in Fig. 5(d) for five packaged dice. An example of a temperature regulation cycle is shown in Fig. 5(e). The measured output power spectrum of the UWB transmitter is plotted in Fig. 5(f).

The SoC was extensively validated in DNA analysis for detection of prostate cancer. Fig. 6(a) shows CV scans of an on-chip Au electrode in a 20μM $K_4[Fe(CN)_6]$ solution. The bare electrode CV scan demonstrates well-defined oxidation and reduction peaks of $K_4[Fe(CN)_6]$. Microelectrodes hybridized with 5μM single-stranded prostate cancer probe DNA show a reduction in the oxidation/reduction peak current due to the increase in the negative surface charge. Adding a 5μM non-complementary target DNA does not significantly change the CV plot indicating that non-specific adsorption is negligible. Adding a 5μM complementary prostate cancer target DNA leads to elimination of $K_4[Fe(CN)_6]$ redox peaks. This is due to the additional negative surface charge resulting from formation of double-stranded DNA on the electrode surface. The 3σ error bars (from 3 chips) with the detection noise margin of approximately 2.34nA are shown in Fig. 6(b).

The die micrograph and a summary of the SoC measured characteristics are depicted in Fig. 7. The 48 channels are arranged in a 8×6 array on a 3mm×3mm 0.13μm CMOS die. Two channel types with different WE configurations are implemented. A set of 42 channels scan 4 WEs each, with three

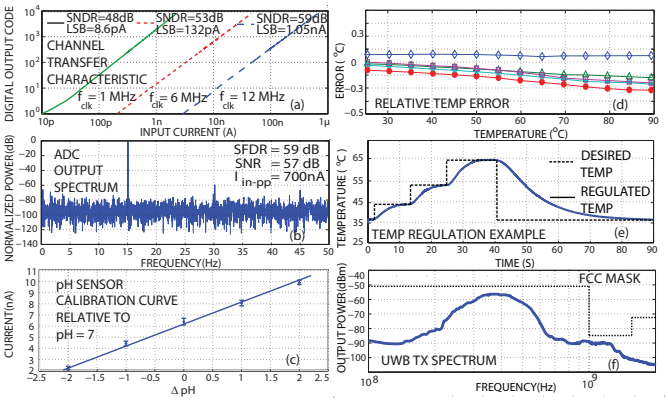

Fig. 5. Experimentally measured results.

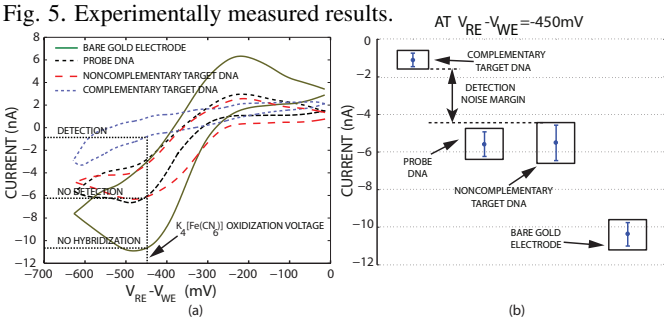

Fig. 6. Experimental on-die prostate cancer DNA detection results.

different WE sizes to cover a 110dB dynamic range, perform initial detection of DNA. A set of 6 channels (in the second bottom row of the array) scan a sub-array of 8×8 2μm×2μm WEs each. These redundant-electrode sub-arrays are utilized for DNA detection cross-validation and for titer DNA concentration measurements.

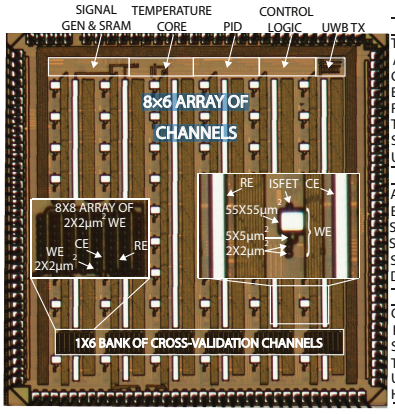

System	
Technology	0.13μm CMOS
Area	3mm×3mm
Channel count	48
Electrode count	576
Regulated temp range	25-90 C
Temp inaccuracy(3σ)	±0.5 C
Signal generator scan rate	400V/s
UWB data rate	10Mb/s
Channel	
Area	300μm× 200μm
Electrode	55×55, 5×5 & 2×2 μm²
Sensitivity	8.6pA
SNR (f_{clk} =12MHz)	78.2dB
SFDR (f_{clk} =12 MHz)	60.1dB
Dynamic range (three f_{clk})	110dB
Power Consumption	
Channel	8μW
PID	21μW
Signal generator	1.1mW (5nF load)
Temperature core	12μW
UWB	100μW @10Mb/s
Heater	270mW @ 90 C

Fig. 7. Die micrograph and experimental results summary.

References

[1]D. M. Garner, B. Hua, P. Georgiou, T. G. Constandinou, S. Reed, L. M. Shepherd, W. Wong, K. T. Lim and C. Toumazou, "A Multi-channel DNA SoC for Rapid Point-of-Care Gene Detection," ISSCC, 2010.

[2]B. Jang, C. Peiyan, A. Chevalier, A. Ellington and A. Hassibi, "A CMOS Fluorescent-Based Biosensor Microarray," ISSCC, 2009.

[3]L. Soleymani, Z. Fang, E. H. Sargent and S. O. Kelley, "Programming Nucleic Acids Detection Sensitivity Using Controlled Nanostructuring," Nature Nanotechnology, Vol. 4, No. 12, 2009.

[4]H. M. Jafari, R. Genov, "CMOS Impedance Spectrum Analyzer with Dual-Slope Multiplying ADC," Biomedical Circuits and System Conference, 2011.

[5]M. A. P. Pertijs, K. Makinwa and J. Huijsing, "A CMOS Smart Temperature Sensor With a 3σ Inaccuracy of $\pm$0.1 ^{o}C From -55 ^{o}C to 125 ^{o}C," ISSCC, 2005.